HOW TO REDUCE SOFI/NTT POLARIMETRIC DATA

S. Wolf[*], L. Vanzi[†], N. Ageorges[‡]

May 17, 2002

[*]California Institute of Technology, 1200 E California Blvd, Mail Code 220-6, Pasadena CA 91125, USA, swolf@ipac.caltech.edu

[†]ESO-Chile, Alonso de Cordova 3107, Vitacura, Santiago, Chile, lvanzi@eso.org

[‡]ESO-Chile, Alonso de Cordova 3107, Vitacura, Santiago, Chile, nageorge@eso.org

Contents

1 Purpose

In this report we describe the use of the polarimetric mode of SOFI for scientific observations. We discuss which calibrations are necessary, how to obtain them, how to carry out the observations, to reduce and to calibrate the data. In particular, the influence and removal of the instrumental polarization (IP) are discussed. For a more detailed description of the polarization mode of SOFI, such as technical aspects, we refer to the "SOFI User's Manual"[1].

The results presented in this report have been obtained from the analysis of the data taken during the technical periods of May, June, and July 2000, February 2001, and February 2002.

This document is mainly directed to the NTT staff performing the instrument calibrations and to the observers that need an advanced knowledge of the subject. The most important results of this work, mainly the information necessary to prepare a proposal and to perform a basic reduction and calibration of polarimetric data of SOFI will be included in the next issue of the "SOFI User's Manual".

[1] http://www.ls.eso.org/lasilla/Telescopes/NEWNTT/sofi/manual/SOFImanual.html

2 Introduction

As in the case of any other (near-infrared) image data reduction, images taken with SOFI at the NTT in polarization mode have to be corrected for "bad" pixels (hot and dead pixels, cosmics, etc.), the sensitivity distribution of the pixels on the chip (flatfield) and the sky contribution:

$$\text{Image} = [(\text{Object} + \text{Sky}) \cdot \text{Flatfield}] + \text{"bad" Pixels} + \text{Noise}. \tag{1}$$

Additionally, one has to consider that

1. The flatfield image may be intrinsically polarized and
2. SOFI/NTT may influence the polarization state of the incoming light (instrumental polarization). The IP may arise from
   (a) A deviation of the transmission of the Wollaston prism for the two beams (whose plane of polarization differs by 90°),
   (b) Reflection on the primary and secondary mirror, and
   (c) The tertiary mirror(M3, Nasmyth feed), where the light is reflected by 45° to the Nasmyth focus.

The main contribution to the instrumental polarization is expexted to arise from (a) and (c). The contributions by (a) and (b) are expected to be constant (for a given wavelength/filter), while the contribution due to the reflection on the mirror M3 is expected to depend on the altitude (parallactic angle) of the telescope. Furthermore, each contribution (a-c) is wavelength-dependent.

3 Observations

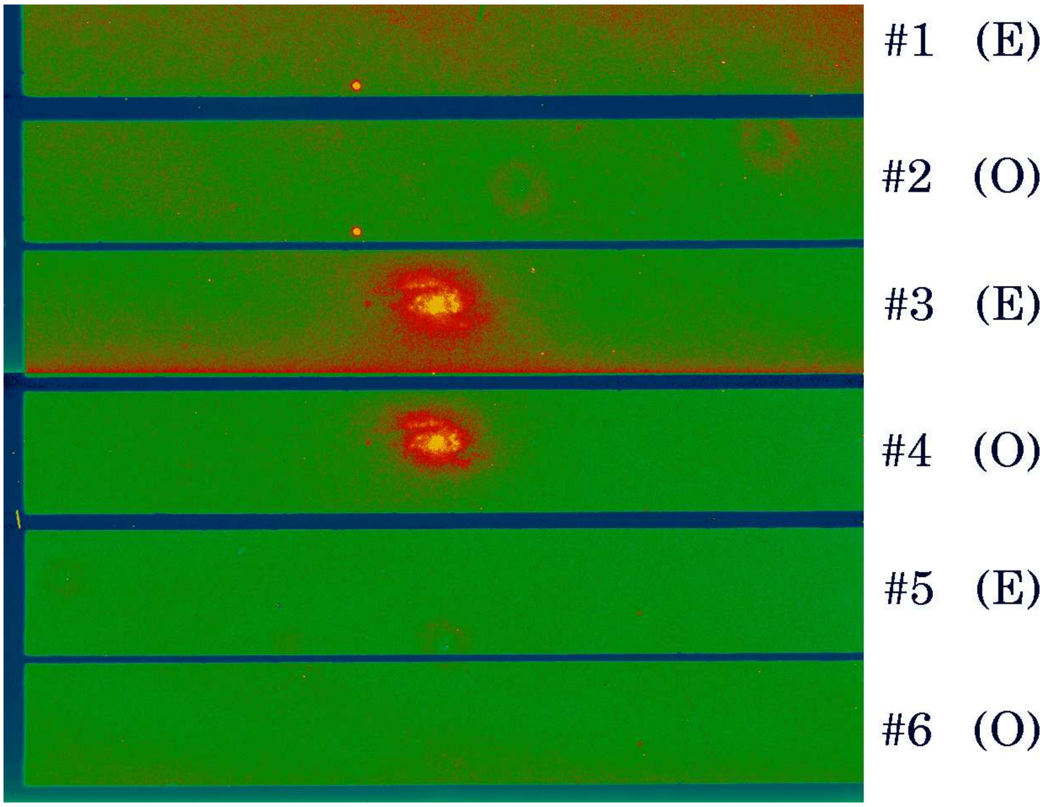

Figure 1: Frame resulting from a single exposure with SOFI using the Wollaston prism and (therefore) the polarimetric mask in the optical path. The two beams are denoted as ordinary ray ("O", component of the incoming light parallel to the axis of the analyser) and extra-ordinary ray ("E", component of the incoming light perpendicular to the analyser axis).

Polarimetric observations performed with SOFI make use of a Wollaston prism. The prism is introduced in the optical path, splitting the incoming light into two beams with perpendicular polarization. Since two images of the observed field are produced on the array it is necessary to limit the field of view of the instrument to avoid overlapping. This is achieved with a special mask (polarimetric mask) that can be inserted in the focal plane of the telescope. The polarimetric mask is mounted on the mask wheel of SOFI, it is made of three open areas about $40'' \times 300''$ in size and three corresponding dark areas (see Fig. 1 for illustration). At least three observations are required to cover the whole field of view of SOFI. The optics used by the polarimetric mode is the same as for the large field so that the pixel scale is unchanged with respect to this mode.

In order to derive the linear polarization degree and orientation of an object, two observations must be performed at each pointing of the telescope with different orientations of the Wollaston prism, typically 0^o and 45^o. These values are defined in the template and correspond to the position angle (PA) on the sky. Doing so, measurements at 0^o and 90^o are obtained at the first observation (orientation of the Wollaston prism: 0^o), while measurements at 45^o and 135^o are obtained at the second (orientation of the Wollaston prism: 45^o). The orientation of the Wollaston prism is changed rotating the whole instrument (SOFI). Furthermore, for each field and for each position angle several images must be acquired offsetting the telescope in order to provide a good sky determination. This is required to achieve a high signal-to-noise ratio (SNR) for the photometric measurements which the polarization quantities are based on. As in the normal imaging, the jitter "ON-ON" is used (keeping the object always in the field) if the object is small enough. When the object is large compared with the size of a single polarimetric mask strip, the jitter "OFF" must be used and an independent sky exposure has to be acquired. The offset pattern develops better in the strip direction in the first case while it is free in the second case. In both cases, the offsets must be explicitely indicated in the template, the auto-jitter mode is not available for the polarimetric mode.

4 Calibration and data reduction

4.1 Badpixel reduction

A map with known dead and hot pixels can be retrieved from `http://www.ls.eso.org/lasilla/Telescopes/NEWNTT/sofi/setup /bad_pix.html`. Furthermore, additional (newer) dead / hot pixels & cosmics have to be removed.

4.2 Flatfield

A flatfield reduction is strongly recommended in order to take into account the sensitivity distribution of the chip. If the flatfield correction is not applied, the photometric error may result in about 2% (Ks band) error of the polarization.

The flatfield exposure should be performed using the same filters as the subsequent object exposures and the Wollaston prism in the optical path. This is important since the flatfield without Wollaston prism may differ substantially from that taken with the Wollaston prism, mainly due to a slightly different illumination of the chip. Since the whole instrument rotates in order to provide a certain orientation of the Wollaston prism, separate exposures at different orientations are not required.

The flatfield f may either me deduced from (1) dome exposures ("dome flatfields"), where a series of exposures with and without a lamp illuminating the inner dome is taken, or (2) the sky map:

1. **Dome flatfields** (*recommended*)

Procedure:	Exposure 1 (e_1):	lamp-off
	Exposure 2 (e_2):	lamp-on (typically 4000 ADU)
	Exposure 3 (e_3):	lamp-on
	Exposure 4 (e_4):	lamp-off

   $$f = (e_2 - e_1) + (e_3 - e_4) \tag{2}$$

   Fig. 2 shows the fields #3 and #4 in case of an exposure with the lamp switched off. The background structure, being typical for SOFI exposures in the polarimetric mode, is due to the infrared background radiation (direct & scattered light) whereby the relative brightness profil is due to the Wollaston and the polarimetric mask in the optical path,

[A]

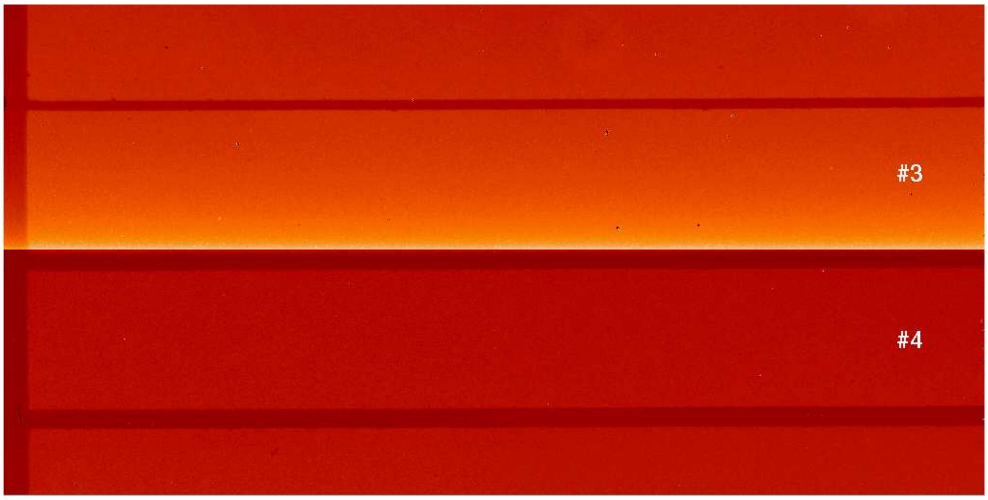

[B]

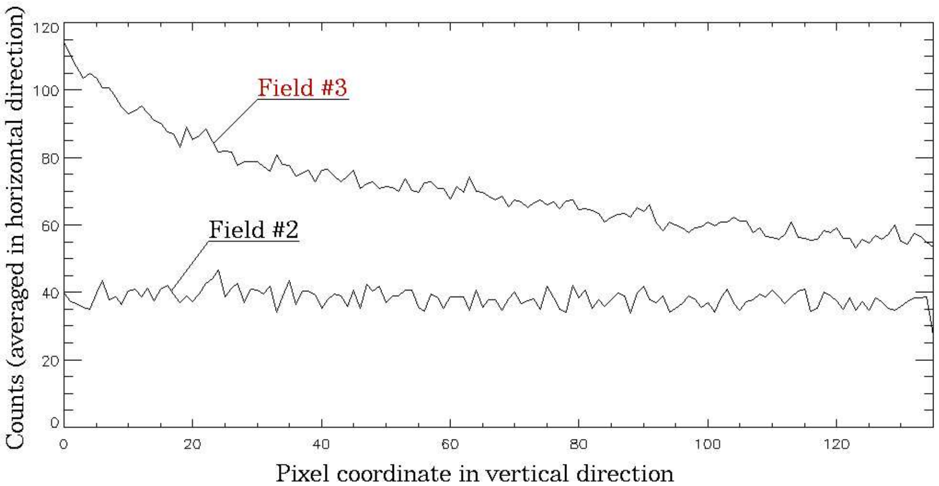

Figure 2: **[A]** Fields #3 and #4 of a dome exposure with the lamp switched off. **[B]** Vertical intensity profile in the upper (#3) and in the lower field (#4), averaged in horizontal direction.

i.e., it appears only in the polarimetric mode and is therefore (in first order) not related to a dark current.

The resulting flatfield image is polarized, i.e., the median value of the upper field is different from the median value of the lower field. However, this problem can be overcome by an independent normalization of the flatfield in each field (see below).

2. **Sky map flatfield**
The flatfield may be deduced from the background sky of many images, if the object was located at different positions on the chip during the measurements. However, it is not recommended because "ghost" images of the object on consecutive images may result in a wrong flatfield especially at the position(s) of the object.

To perform the flatfield reduction, we recommend the following procedure (in the following is assumed that the object does not exceed the size of a single field[2] of 5'×0.7'):

1. Create a flatfield for each of the two fields on the detector. Let f_{u} (f_{l} be the upper (lower) flatfield.

2. Select the upper/lower field from the flatfield f (take care not to get in the range blended by the mask; see Fig. 3): $f_{\mathrm{u},0}$, $f_{\mathrm{l},0}$.
Rem.: Measurements in the Ks band show that the change of the flatfield polarization within $f_{\mathrm{u},0}$, $f_{\mathrm{l},0}$ is not zero but less than 0.05% and therefore negligible compared to the other sources of error. Therefore, the assumption that no pixel-to-pixel polarization in $f_{\mathrm{u},0}$, $f_{\mathrm{l},0}$ exists, is valid.

3. Normalize each flatfield:

$$f_{\mathrm{u},1} = \frac{f_{\mathrm{u},0}}{\mathrm{median}(f_{\mathrm{u},0})}, \tag{3}$$

$$f_{\mathrm{l},1} = \frac{f_{\mathrm{l},0}}{\mathrm{median}(f_{\mathrm{l},0})}. \tag{4}$$

[2] In the following, the two central fields harbouring the object (#3 and #4 in Fig. 1) are refered to as the “upper” and “lower” field.

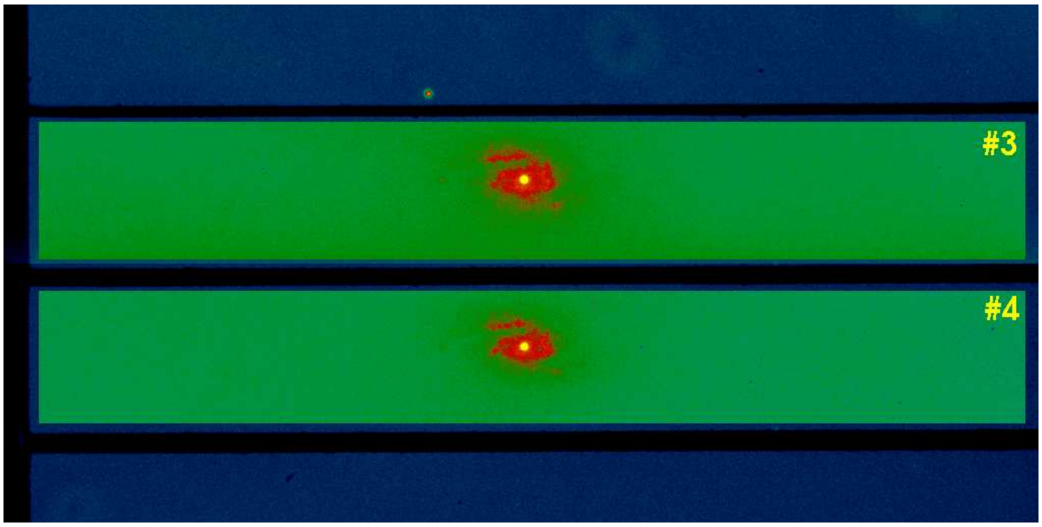

Figure 3: Areas considered in the flatfield for the data reduction considered in this article (highlighted areas; *recommended*). These areas have the pixel coordinates $[x_{\rm min} : x_{\rm max}, y_{\rm min} : y_{\rm max}]$=[35:1010,516:651] (upper field) and [35:1010,354:484] (lower field).

4. Divide the upper/lower field of the (object) image ($i_{\rm u}$) by the corresponding flatfield:

$$i_{\rm u,1} = \frac{i_{\rm u,0}}{f_{\rm u,1}}, \tag{5}$$

$$i_{\rm l,1} = \frac{i_{\rm l,0}}{f_{\rm l,1}}. \tag{6}$$

This way, the flatfield correction can be done without introducing an artificial polarization due to a possible intrinsic polarization of the flatfield. This procedure is based on the assumption that if the flatfield is polarized, the polarization (degree and orientation) is constant over the whole field of 5'×0.7' (= area of the upper [lower] field), i.e., the pixel-to-pixel polarization is negligible as stated above.

4.3 Correction for the wrong transmission ratio of the Wollaston prism

A further artificial polarization is introduced due to a deviation of the transmission ratio of the Wollaston prism (ideal: 50%:50% = intensity upper:lower beam). The following three alternatives for the correction of the wrong transmission ratio are proposed:

1. Use the factor of $C_{\mathrm{Ks}} = 0.968$ (Ks band) and $C_{\mathrm{J}} = 0.954$ (J band), respectively (see App. B for details):

$$i_{\mathrm{u},2} = i_{\mathrm{u},1} * C, \tag{7}$$

$$i_{\mathrm{l},2} = i_{\mathrm{l},1}. \tag{8}$$

2. Since the sky is also affected by this effect, a good measure for the intensity ratio of both beams can be derived from the median of the lower/upper image:

$$i_{\mathrm{u},2} = i_{\mathrm{u},1} * \frac{\mathrm{median}(i_{\mathrm{l},1})}{\mathrm{median}(i_{\mathrm{u},1})}, \tag{9}$$

$$i_{\mathrm{l},2} = i_{\mathrm{l},1}. \tag{10}$$

   This method may not be applied if the polarized object covers a large fraction of the lower/upper image (because then the median value may be influenced by the possibly polarized object).
   Problem: This method works properly only if the background radiation of the sky is unpolarized and the images are not affected by scattered moonlight.

3. Fitting a $\cos(2\theta)$ function to the intensity of the object on the image as a function of the orientation (θ) of the wollaston prism (see Ageorges 2000).

4.4 Sky substraction

Since the intensity of the background radiation (and also its components after passing the Wollaston prism) is an *additive* component to the intensity

of the object, the substraction of the sky will also result in the removal of the contribution of the sky polarization to the net polarization of the object. Therefore, the sky has to be estimated and substracted independently for both the upper and the lower field.
Methods:

1. Substract the median of each field from the corresponding field.
    - *Assumption*: No sky variation within the image area.
    - It may be applied only if the image is dominated by the sky, since the median of the image would be remarkably higher than the sky if the image is crowded by stars or a large fraction of the image is covered by an extended object.
2. If the object was taken at different positions on the detector ("Dithering technique"), and the sky was stable (no clouds, etc.) during the exposures.
    (a) Let the sky value of a pixel in a particular image be the *median* value of this pixel in all images.
    - The resulting sky frame is the same for each image.
    - It may only be applied if the number of images (= number of different positions of the object on the chip) is large enough ($>$ 5 exposures recommended). Otherwhise, the resulting sky intensity at each position of the object is too high.

    (b) Let the sky of a pixel in a particular image be the *mean* value of this pixel in all other images
    - This results in indivual sky frames for each image.

    (c) Let the sky of a pixel in a particular image be the *minimum* value of this pixel in all images
    - Again, this results in individual sky frames for each image.
    - It is not recommended since the contribution of the sky will be systematically underestimated.

    Common aspects of method (a) and (b):
    - The quality of sky frames increases with the number of individual images.

- Any overlay of the regions covered by the object on individual exposures must be prevented.
- Both methods are equally good, i.e., between the resulting difference between the resulting sky frames is much smaller than the statistical error of the photometry. However, method (b) is faster.

Additionally one may verify and, if necessary, correct the removal of the local sky background by fitting a bi-dimensional polynome to the background measured in areas free of cosmic rays and faint objects. Polynomes of the first degree have been found to produce the best results.

5 Polarization

5.1 Stokes Parameters

Based on two orientations of the Wollaston prism (usually 0° and 45°) the concept of the Stokes vector for determination of the linear polarization degree and orientation can be applied. The three components of the Stokes vector required for this (I,Q,U)[3] are defined as follows:

$$I = I_0 + I_{90} = I_{45} + I_{135}, \tag{11}$$

$$Q = I_0 - I_{90}, \tag{12}$$

$$U = I_{45} - I_{135} \tag{13}$$

Here I_0, I_{90}, etc., are the intensities of the object at the corresponding polarization direction (0°, 90°, etc.). Hereby, the orientation (angle) of the lower field's polarization is that of the Wollaston prism. The polarization direction of the upper field differs by 90° from this (see Fig. 4).

Definition of the *normalized Stokes parameters*:

$$q = \frac{Q}{I} \tag{14}$$

and

$$u = \frac{U}{I}. \tag{15}$$

5.2 Correction for Instrumental Polarization

The remaining IP is expected to be mainly caused by the reflection on the tertiary mirror M3. It should therefore depend on the altitude angle of the telescope. However, the remaining IP was found to be $< 0.3\%$ (Ks band) and $< 0.4\%$ (J band) in our investigation, respectively (see App. B). Since the (statistical) error of the results from which these limits have been derived is in the same order of magnitude, a possible contribution by the mirror M3 could not be extracted.

[3]The "complete" Stokes is contains a further parameter, usually denoted as "V", which allows to consider the circular polarization as well. See, e.g., Collett (1993) for an introduction into the concept of the Stokes vector.

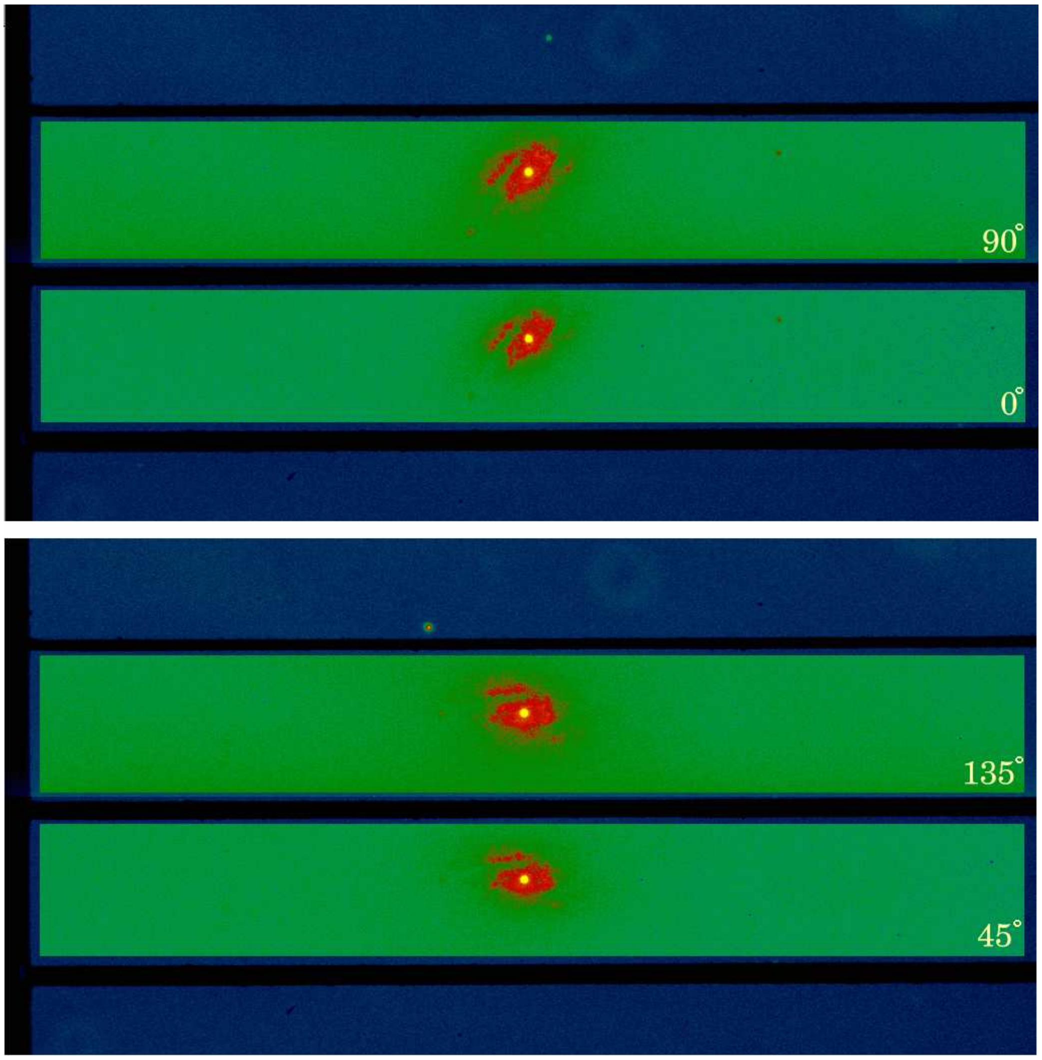

Figure 4: Orientation of the Wollaston prism and resulting preferential direction of the electric field vector of the light projected on the two inner fields of the chip (#3 and #4).

5.3 Orientation and degree of the linear polarization

The degree (P) and orientation (γ) of the linear polarization can be derived on two ways:

1. Using the (normalized) Stokes parameters:
$$P = \sqrt{q_{\text{object}}^2 + u_{\text{object}}^2} \tag{16}$$
and
$$\gamma = \frac{1}{2}\text{atan}\left(\frac{u_{\text{object}}}{q_{\text{object}}}\right). \tag{17}$$

2. Alternatively, the polarization degree and orientation can be derived from the polarization curve (intensity of the object as a function of the polarization direction of the Wollaston prism).

In both cases, an oversampling by measuring the intensity (difference) for more than two orientations of the Wollaston prism increases the accuracy of the polarization measurement.

If the polarization measurement is based on the determination of the Stokes parameters q and u, measurements for a pair (two) of orientations of the Wollaston prism differing by 45$^{\text{o}}$ are also required. If ε_0 is the (arbitrary) initial orientation of the Wollaston prism, the polarization can be derived from:

$$q' = \frac{I(\varepsilon_0) - I(\varepsilon_0 + 90^{\text{o}})}{I(\varepsilon_0) + I(\varepsilon_0 + 90^{\text{o}})}, \tag{18}$$

$$u' = \frac{I(\varepsilon_0 + 45^{\text{o}}) - I(\varepsilon_0 + 135^{\text{o}})}{I(\varepsilon_0 + 45^{\text{o}}) + I(\varepsilon_0 + 135^{\text{o}})}, \tag{19}$$

$$P = \sqrt{q'^2 + u'^2}, \tag{20}$$

and

$$\gamma = \frac{1}{2}\ \text{atan}\left(\frac{u'}{q'}\right) + \varepsilon_0. \tag{21}$$

5.4 Take many exposures!

Using the definition of the polarization degree based on the Stokes parameters I, Q, and U (see Eq. 11–16), for a single polarization measurement, i.e., two exposures of the object with the Wollaston prism at two orientations differing by 45°, it is a reasonable assumption that the abolute errors of the Stokes parameters are given by

$$\Delta Q \approx \Delta U \approx \Delta I \approx 2\Delta I', \tag{22}$$

where $\Delta I'$ is the absolute error of a single photometric measurement. Then, the absolute error of the polarization degree can approximately written as

$$\Delta P \approx \left[2 \ldots 2\left(1+\sqrt{2}\right)\right] \frac{\Delta I'}{I}, \tag{23}$$

where the amount of the coefficient depends on the polarization degree and the amount of the ratio $Q/U = q/u$. Thus, the *absolute* error of the polarization measurement is directly related to the *relative* photometric error! The orientation of the linear polarization γ is even more sensitive to the accuracy of the photometric measurement and the degree of the polarization:

$$\sigma_\gamma = \frac{\sqrt{(q\ \sigma_\mathrm{q})^2 + (u\ \sigma_\mathrm{u})^2}}{P^2}, \tag{24}$$

which is valid for $P \gg \sigma_\mathrm{P}$ (σ_γ, σ_q, and σ_u are the standard deviations of the orientation of polarization and the reduced Stokes parameters q and u; see Sect. D). Since the net polarization of many astrophysical objects does not exceed a few percent, the required accuracy can be achieved often only on the basis of a large number of (dithered) exposures (see Sect. D for particular error estimates for series of exposures).

The polarization pattern of spatially resolved objects on the other hand, such as the circumstellar shells around young stellar objects and galaxies, show (locally) high polarization degrees. Thus, these measurements are much less effected and easier to perform. Furthermore, the SNR can be drastically increased, in particular by a factor of n, if areas of $n \times n$ pixels are combined. The main difficulty in case of extended objects is to find a correct superposition (a) of dithered images obtained with the Wollaston prism at the same position and (b) of the co-added exposures obtained at the different orientation of the Wollaston prism. In Fig. 5 the polarization pattern of the Circinus galaxy obtained with SOFI is shown as an example.

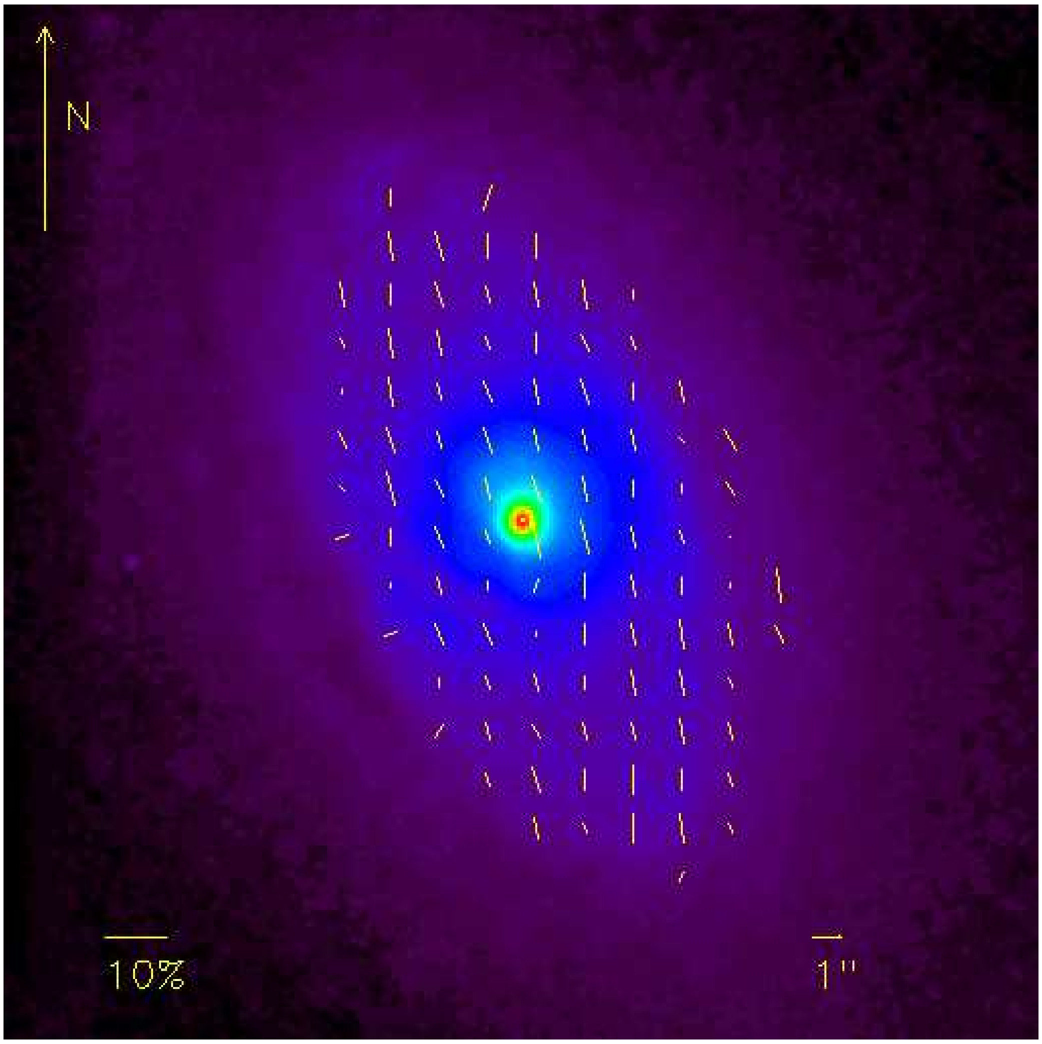

Figure 5: Polarization pattern of the Circinus galaxy obtained with SOFI/NTT on May 5, 2000. 12 exposures $\times$ 2 orientations of the Wollaston prism have been used (Filter: NB CO). Only polarization vectors with $P > 5\sigma_{\mathrm{P}}$ are shown.

References

[1] Ageorges N., *"Description of the reduction of the SOFI polarimetric data"*, `http://www.eso.org/ nageorge/sofipola.html`, Technical report, ESO, 2000

[2] Collett, E., "Polarized light", Marcel Dekker, Inc.: New York, Basel, 1993

[3] Gehrels T., "Planets, Stars & Nebulae studied with Photopolarimetry", University of Arizona Press Tucson, 1974

[4] Lamy H., Hutsemekers D., *"A procedure for linear polarization measurements"*, The Messenger 96, 25, 1999

[5] Lidman C., Cuby J.-G., Vanzi L., Hainaut O., Melnick J., *"SOFI, User's Manual"*, Issue 1.3, `http://www.ls.eso.org/lasilla/Telescopes/NEWNTT/sofi/manual/SOFImanual.html`, La Silla Observatory, 2000

[6] Nagata T., *"Observation of interstellar polarization at 2.2 and 3.8 microns"*, ApJ 348, L13, 1990

[7] Turnshek D.A., Bohlin R.C., Williamson II R.L., Lupie O.L., Koornneef J. *"An atlas of Hubble Space Telescope photometric, spectrophotometric, and polarimetric calibration objects"*, AJ 99, 1243, 1990

[8] Walsh J., *"SOFI Polarimetry Mode - Instrumental Polarization"*, `http://www.stecf.org/~jwalsh/SOFIinspol.html`, Technical Report, ESO, 1997-1999

[9] Wardle J.F.C., Kronberg P.P., *"The linear polarization of quasi-stellar radio sources at 3.71 and 11.1 centimeters"*, ApJ 194, 249, 1974

[10] Whittet D.C.B., Martin P.G., Hough J.H., Rouse M.F., Bailey J.A., Axon D.J. *"Systematic variations in the wavelength dependence of interstellar linear polarization"*, ApJ 386, 562, 1992

A Catalogues of polarized/unpolarized standard stars

1. Unpolarized Polarization Standard Stars:
   see `http://www.jach.hawaii.edu/JACpublic/UKIRT/instruments/irpol/irpol_stds.html#Unpolarized`

2. "Serkowski" Polarization Standard Stars:
   see `http://www.jach.hawaii.edu/JACpublic/UKIRT/instruments/irpol/irpol_stds.html#Serkowski`

3. Polarized Stars from Whittet et al. (1992):
   see `http://www.jach.hawaii.edu/JACpublic/UKIRT/instruments/irpol/irpol_stds.html#Whittet`

4. Polarized and Unpolarized Polarization Standard Stars:
   Turnshek D.A., et al., AJ 99, 1243, 1990

B HD 64299

This polarization standard star was chosen to *develope* the data reduction procedure presented in this work (including the investigation of the instrumental polarization). Furthermore, additional observations of unpolarized polarization standard stars (HD 94851, HD 94851, HD 98281, HD 98161, HD 125184) have been used to verify the reduction procedure and to enforce the conclusion made about the the IP, i.e., the transmittance of the Wollaston prism. The main parameters of the considered polarization standard stars and their observations are compiled in Tab. B.

Assuming that the polarization of this star is mainly determined by interstellar polarization, the expected J/Ks band polarization is $P(\mathrm{J}) \approx 0.05\%$ / $P(\mathrm{Ks}) \approx 0.03\%$ (see, e.g., Nagata 1990). Since these values are smaller than the polarization accuracy achievable with SOFI, the polarization of this star is negligible in the following discussions.

Observations:
The object was mapped in the Ks and the J band at orientations of the Wollaston prism of 0^o, 22.5^o, 45^o, and 67^o degree at following altitude angles of the telescope: 24^o, 26^o, 32^o, 41^o, 54^o, 64^o, 68^o, 72^o, and 83^o. In each case, three exposures have been taken with a constant offset in right ascension between consecutive exposures (offset: 40").

Applied reduction steps:

1. Bad pixel reduction,
2. Flatfield correction: (a) dome flatfields,
3. No correction for wrong transmission of the Wollaston prism,
4. Sky substraction: (a) from individual image,
5. Estimation of the (relative) intensities I_{90}, etc. of the object (see below).

No correlation between the measured polarization degrees and the altitude of the telescope and the orientation of the Wollaston prism was found. The

HD 64299	Right Ascension	$07^{\mathrm{h}} : 52^{\mathrm{m}} : 25.55^{\mathrm{s}}$
	Declination	$-23^{\mathrm{o}} : 17' : 45.9''$
	Epoch	J2000.0
	P(B)	0.151±0.032%
	m_{V}, Spectral type	10.15, A2V
	Reference	Turnshek et al. (1990)
HD 94851	Right Ascension	$10^{\mathrm{h}} : 56^{\mathrm{m}} : 44.17^{\mathrm{s}}$
	Declination	$-20^{\mathrm{o}} : 39' : 51.6''$
	Epoch	J2000.0
	P(B)	0.057±0.018%
	m_{V}, Spectral type	9.10, B9
	Reference	Turnshek et al. (1990)
HD 98281	Right Ascension	$11^{\mathrm{h}} : 15^{\mathrm{m}} : 49.2^{\mathrm{s}}$
	Declination	$-04^{\mathrm{o}} : 47' : 37''$
	Epoch	B1950.0
	m_{V}, Spectral type	7.30, G8V
	Reference	Gehrels (1974)
HD 98161	Right Ascension	$11^{\mathrm{h}} : 17^{\mathrm{m}} : 11.84^{\mathrm{s}}$
	Declination	$-38^{\mathrm{o}} : 00' : 52.0''$
	Epoch	J2000.0
	P(B)	0.017±0.06%
	m_{V}, Spectral type	6.27, A3V
	Reference	Turnshek et al. (1990)
HD 125184	Right Ascension	$14^{\mathrm{h}} : 15^{\mathrm{m}} : 21.1^{\mathrm{s}}$
	Declination	$-07^{\mathrm{o}} : 18' : 32''$
	Epoch	B1950.0
	m_{V}, Spectral type	6.5, G8V
	Reference	Gehrels (1974)

Table 1: Parameters of the considered polarization standard stars.

derived polarization degree and orientation are[4]:

$$\begin{array}{lcl} P(\mathrm{Ks}) & = & 2.05 \pm 0.43\,\% \quad , \quad \gamma = 115 \pm 6^{\circ}, \\ P(\mathrm{J}) & = & 3.11 \pm 0.62\,\% \quad , \quad \gamma = 116 \pm 6^{\circ}. \end{array} \tag{25}$$

Here, the (relative) intensities of the object have been estimated by two different methods:

1. - Fitting a Gaussian profil to each object image
   - Integrating the intensity within an aperture with a radius of

     $$R = n_\sigma * \sigma, \tag{26}$$

     whereby

     $$\sigma = \frac{1}{\sqrt{2 \ln 2}} \, \frac{\sigma'}{2}. \tag{27}$$

     Here, σ' is the FWHM of the Gaussian profil and in agreement with the investigation of Lamy & Hutsemekers (1996) concerning polarimetric measurements with EFOSC2 at the ESO 3.6-m telescope, $n_\sigma \approx 2.5$ was found to define an optimum area of integration.
   - The integration was performed on sub-pixel scale. In this context it was found that for a sufficient integration each pixel has to be divided into a field of $\geq 10{\times}10$ sub-pixels.
2. Integration inside an aperture with a fixed radius (corresponding to the seeing dominated size of the object, radii of 5, 6, and 10 Pixels have been chosen).

Before each integration it was verified that the median intensity of the "local" sky around the object was zero (the radius of the local sky around the object was chosen 4...8 times larger than the integration area of the object). The results of both routines (and the different integration areas applied in the second method) are equal within the error intervals.

Under the *assumption* that the measured polarization is mainly determined by the different efficiency of the Wollaston prism for the two polarization directions, following correction factors for the ratio of the intensities measured in the lower/upper field have been derived:

[4]The estimation of the polarization error intervals is based on the work of Wardle & Kronberg (1974, see App. D).

$$\begin{array}{lcccccc} \mathrm{J} & : & C_{\mathrm{J}} & = & 0.954 & \pm & 0.006, \\ \mathrm{Ks} & : & C_{\mathrm{Ks}} & = & 0.968 & \pm & 0.007. \end{array} \tag{28}$$

The error intervals include the values being derived for the different orientations of the Wollaston prism (see also Fig. 3 in Ageorges 2000; consider that the correction factor provided there is based on the inverse intensity ratio compared to the values discussed here). The lower-to-upper intensity ratios of the single exposures of HD 64299 and further unpolarized polarization standard stars (see Tabl. B), taken at an orientation of 0^{o} and 45^{o}, are shown in Fig. 6.

Discussion:
The small, statistically distributed[5] variations of the correction factors, derived for exposures obtained for different altitudes of the telescope and different orientations of the Wollaston prism, confirm the assumption given above, i.e., the IP is determined by the wrong transmission ratio of the Wollaston prism. If – in contrast to this – the measured polarization was due to reflections on the mirrors of the telescope, the intensity ratio between the object in the upper and the lower field would depend on the orientation of the Wollaston prism. Furthermore, it was expected to depend on the altitude of the telescope if the mirror M3 was a significant source of IP. Here, the opposite behaviour was found: The modification of the polarization of the light due to reflection occuring *before* the light passes the Wollaston prism is negligible compared to the effect of the different effiencies of the Wollaston prism for the two polarization directions.

The derived polarization of the unpolarized polarization standard star HD 64299 after the correction of the different transmission efficiencies of the Wollaston prism are:

$$\begin{array}{lccccc} P(\mathrm{J}) & = & (0.36 & \pm & 0.21)\,\%, \\ P(\mathrm{Ks}) & = & (0.31 & \pm & 0.25)\,\%. \end{array} \tag{29}$$

Due to the large σ_{P}/P ratio, it is not possible to derive the remaining IP. Thus, the polarizations given above are upper limits for the (remaining) IP.

[5] Normal Distribution.

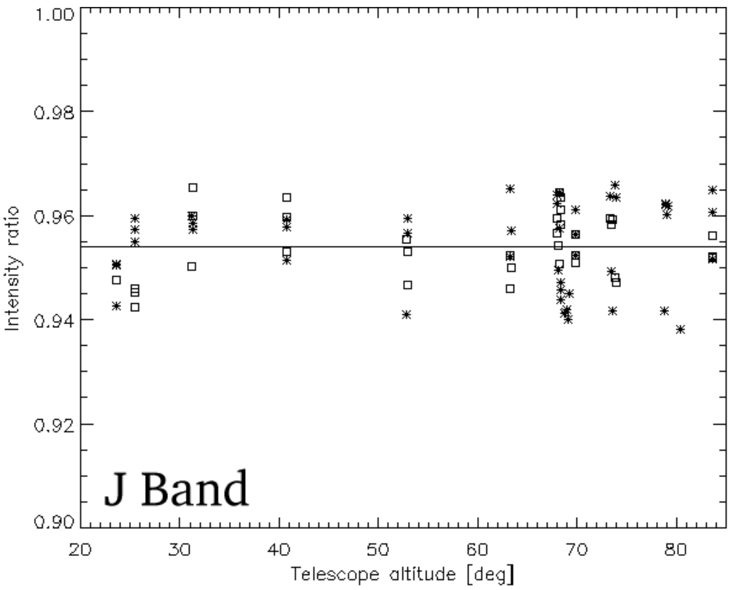

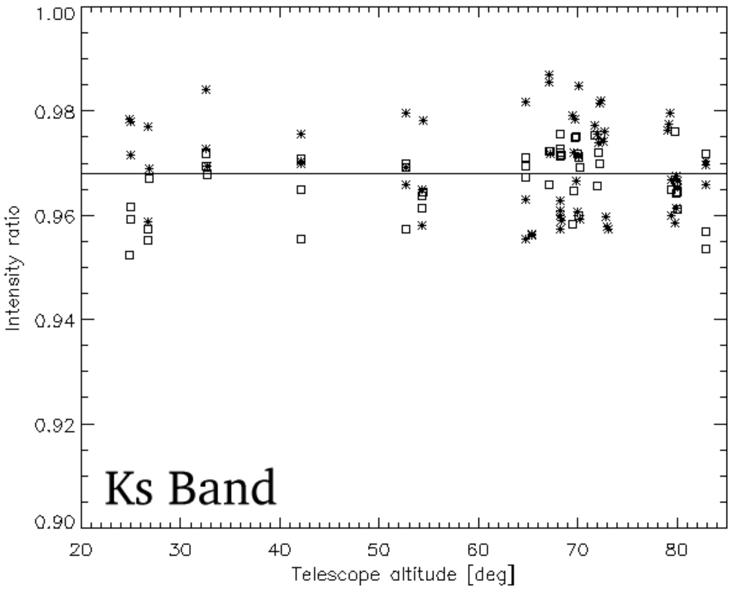

Figure 6: Upper-to-lower intensity ratio in the J and Ks band of the considered unpolarized polarization standard stars derived from single exposures. The asterisks symbolize the intensity ratios obtained at an orientation of 0^o of the Wollaston prism, while the open squares represent the ratios obtained at a 45^o orientation.

C Elias 14 (r Oph)

This (polarized) polarization standard star was chosen to *test* the data reduction procedure presented in this work. Its parameters are given in Tabl. C.

The object was mapped in the Ks and the J band at orientations of the Wollaston prism of $0^{\rm o}$ and $45^{\rm o}$ at following altitude angles of the telescope: $19^{\rm o}$, $28^{\rm o}$, $42^{\rm o}$, and $52^{\rm o}$. In each case four exposures have been taken with a constant offset in right ascension between consecutive exposures (offset: 25"). Since the object was very bright, the exposures have been taken with the telescope being strongly defocussed.

$$
\begin{array}{lcl}
P(\mathrm{Ks}) & = & 2.01 \pm 0.48\,\%, \quad \gamma = 8 \pm 7^{\rm o}, \\
P(\mathrm{J}) & = & 5.06 \pm 0.43\,\%, \quad \gamma = 6 \pm 4^{\rm o}.
\end{array}
\tag{30}
$$

The derived polarization degrees and orientations agree with the values from the literature (within the error interval).

Elias 14	Right Ascension	$16^{\rm h} : 23^{\rm m} : 01.7^{\rm s}$
	Declination	$-24^{\rm o} : 16' : 50''$
	Epoch	B1950.0
	$P(\mathrm{Ks})$	$1.95 \pm 0.03\,\%$
	$\gamma(\mathrm{Ks})$	$3 \pm 1^{\rm o}$
	$P(\mathrm{J})$	$4.95 \pm 0.02\,\%$
	$\gamma(\mathrm{J})$	$2 \pm 1^{\rm o}$

Table 2: Parameters of the polarization standard star Elias 14 (r Oph); from Whittet et al. (1992).

D Estimation of the error intervals

Following the work by Wardle and Kronberg (1974), standard deviation of the degree and the orientation of the linear polarization ($\sigma_{\rm P}$ and σ_γ) can be derived as follows:

$$\sigma_{\rm P} = \frac{\sqrt{(q\ \sigma_{\rm q})^2 + (u\ \sigma_{\rm u})^2}}{P} \tag{31}$$

and

$$\sigma_\gamma = \begin{cases} 29^{\rm o}\ \frac{\sigma_{\rm P}}{P} & : \ P \gg \sigma_{\rm P} \\ 52^{\rm o} & : \ P \approx 0 \end{cases} . \tag{32}$$

In this work the criterion $P > 3\,\sigma_{\rm P}$ was applied (corresponding to the case $P \gg \sigma_{\rm P}$ in Eq. 32). The value of $\sigma_\gamma = 52^{\rm o}$ in the case $P \approx 0$ results from the equipartition of the polarization angles within the interval $[0^{\rm o}, 180^{\rm o}]$ in that case (exact value for $P = 0$: $[30\sqrt{3}]^{\rm o}$).

If the polarization degree is derived from several individual measurements and $\bar{P}$ is the arithmetic mean of these polarization degrees, correct polarization degree is derived from

$$P = \sqrt{\bar{P}^2 - \sigma_{\rm P}^2}. \tag{33}$$

This correction, which is necessary since the polarization degree is a positiv value, does not have to be applied if the polarization degree was derived from the (arithmetic) mean of the Stokes parameters.